Article

Dynamic complexity in a discrete-time predator-prey system with Michaelis-Menten functional response: Gompertz growth of prey

Sarker Md. Sohel Rana
University of Dhaka, Dhaka-1000, Bangladesh
E-mail: srana.mthdu@gmail.com

Received 24 January 2020; *Accepted 29 February 2020*; *Published 1 September 2020*

Abstract

A discrete-time predator-prey system with Michaelis-Menten functional response and Gompertz growth of prey is examined to reveal its chaotic dynamics. We prove algebraically that when one of the model parameter passes its critical value, the system passes through a flip bifurcation (FB) and Neimark-Sacker bifurcation (NSB) in the interior of $\mathbb{R}^2_+$. We apply the center manifold theorem and bifurcation theorems to determine the existence conditions and direction of bifurcations. Numerical simulations are employed which include the diagram of bifurcations, phase portraits, periodic orbits, invariant cycle, abrupt emergence of chaos, and attracting chaotic sets. In addition, maximum Lyapunov exponents (MLEs) and fractal dimension (FD) are computed numerically to justify the existence of chaos in the system. Finally, we apply feedback control method to control chaotic trajectories.

Keywords predator-prey system with Michaelis-Menten functional response; Gompertz growth; bifurcations; Lyapunov exponents; feedback control.

Computational Ecology and Software
ISSN 2220-721X
URL: http://www.iaees.org/publications/journals/ces/online-version.asp
RSS: http://www.iaees.org/publications/journals/ces/rss.xml
E-mail: ces@iaees.org
Editor-in-Chief: WenJun Zhang
Publisher: International Academy of Ecology and Environmental Sciences

1 Introduction

Mathematical modeling is a promising approach to understand and analyze the dynamics of ecological systems. Many mathematical models have been developed to interpret the interaction between the species. One can describe the dynamics of population growth if the functional behavior of growth rate is known. Eventually, this functional behavior is measured in the laboratory or in the field. In population ecology, the interaction between predator and prey species play fundamental role and have long been studied one of the dominant themes due to their universal existence and importance (Berryman, 1992). Different predator-prey models can be found in the literature (Berryman, 1992; May, 1974). The most studied mathematical model describing a predator-prey interaction is the following well-known Kolmogorov type predator-prey model with Michaelis-Menten (or Holling type II) functional response (Freedman, 1980; May, 1974):

$$\begin{aligned} \dot{x} &= g(x,K) - \frac{\alpha x}{a+x}\, y \\ \dot{y} &= \frac{\beta x}{a+x} y - dy \end{aligned} \tag{1}$$

where $g(x,K) = rx\left(1-\frac{x}{K}\right)$; x and y stand densities of prey and predator, respectively; $r, K, a, \alpha, \beta, d$ are all positive constants that stand for intrinsic growth rate of the prey, the carrying capacity of the prey, half saturation constant, capturing rate of prey, maximal growth rate of predator, the mortality rate of the predator, respectively. In (1), prey grows logistically if predator is absent. The qualitative analysis of solutions for system (1) is well established (Freedman, 1980; May, 1974). To investigate the dynamics of a community comprising of population of various interacting species, Gompertz, 1825,developed an alternative expression for the prey birth rate which is similar in effect to logistic growth: $g(x,K) = rx\ln\left(\frac{K}{x}\right)$.

Though most predator-prey theories are based on continuous models governed by differential equations, in recent year, a number of famous ecologist and mathematician have been paid attention and investigated extensively the discrete version of continuous-time models. Because if population size is small, or population generations are relatively discrete (non overlapping), studies on discrete predator-prey model is more appropriate rather than continuous model as discrete-time model reveals very rich and complex dynamics. Besides, for insects with non-overlapping generations, predator-prey system can be modeled in a discrete-time form and numerical computation also requires to discretize a continuous-time model (He and Lai, 2011; He and Li, 2014; Rana, 2015, 2017, 2019; Liu and Cai, 2019; Zhao et al., 2016; Zhao et al., 2017). These researches found many complex properties including attracting fixed point, stable orbits, periodic, quasi-periodic and non-periodic orbits through the possibility of flip and Neimark-Sacker bifurcations which had been derived either by numerically or by normal form and center manifold theory.

In this paper, we consider the following predator-prey system with Gompertz growth of prey:

$$\begin{aligned} \dot{x} &= rx\ln\left(\frac{K}{x}\right) - \frac{\alpha x}{a+x}\, y \\ \dot{y} &= \frac{\beta x}{a+x} y - dy \end{aligned} \tag{2}$$

To get following two-dimensional discrete system, forward Euler scheme with integral step size δ is applied to system (2):

$$\begin{pmatrix} x \\ y \end{pmatrix} \mapsto \begin{pmatrix} x + \delta\left[rx\ln\left(\frac{K}{x}\right) - \frac{\alpha x}{a+x}\, y\right] \\ y + \delta\left[\frac{\beta x}{a+x} y - dy\right] \end{pmatrix} \tag{3}$$

The objective is to see how model parameters affect on the dynamics of system (3).Especially, we discuss systematically the existence condition of flip and NS bifurcation bifurcations in the interior of $\mathbb{R}^2_+$ using bifurcation theory and center manifold theory (Kuzenetsov, 1998). Because in the discrete predator-prey system, these two bifurcations are the main mechanisms to produce complex dynamics and cause the system to jump from stable to unstable states and trigger a route to chaos via periodic and quasi-periodic states.

This paper is organized as follows. Section 2 presents the existence condition for fixed points of system (3) and their stability criterion. In Section 3, the direction of bifurcation for system (3) under certain parametric condition is determined. The diagrams of bifurcation, phase portraits, maximum Lyapunov exponents and

Fractal dimensions of the system (3) for one or more control parameters are presented in Section 4 by implementing numerical simulations. In Section 5, we apply the feedback control method to stabilize chaos at unstable trajectories. Finally a short discussion is carried out in Section 6.

2 Existence Conditions and Stability Analysis of Fixed Points

2.1 Fixed points and their existence

For all permissible parameters value, a simple algebraic computation shows that the model system (3) possesses the following two fixed points:

i. The boundary fixed point $E_1(K,0)$. Biologically it presents that in the absence of predators, the prey population reaches in the carrying capacity,

ii. The unique coexistence fixed point $E_2(x^*,y^*)$ where $x^* = -\frac{ad}{d-\beta}$ and $y^* = -\frac{ar\beta \mathrm{Log}\left[\frac{K(-d+\beta)}{ad}\right]}{\alpha(d-\beta)}$ and exists if $\beta - d > \frac{ad}{K}$.

2.2 Dynamical behavior: stability analysis

We analyze local stability of system (3) at each fixed points by computing the magnitude of eigenvalues of Jacobian matrix evaluated at fixed point $E(x,y)$. The Jacobian matrix of system (3) around fixed point $E(x,y)$ is given by

$$J(x,y) = \begin{pmatrix} j_{11} & j_{12} \\ j_{21} & j_{22} \end{pmatrix} \tag{4}$$

where

$$\begin{aligned} j_{11} &= 1 - r\delta - \frac{ay\alpha\delta}{(a+x)^2} + r\delta \ln\left(\frac{K}{x}\right), \\ j_{12} &= -\frac{x\alpha\delta}{a+x}, \\ j_{21} &= \frac{ay\beta\delta}{(a+x)^2}, \\ j_{22} &= 1 - d\delta + \frac{x\beta\delta}{a+x}. \end{aligned} \tag{5}$$

The characteristic equation of matrix J is

$$\lambda^2 + p(x,y)\lambda + q(x,y) = 0 \tag{6}$$

where $p(x,y) = -trJ = -(j_{11} + j_{22})$ and $detJ = j_{11}j_{22} - j_{12}j_{21}$.Using Jury's criterion (Elaydi, 1996), we state the following stability conditions of fixed points.

Proposition 2.1 *For the boundary fixed point $E_1(K,0)$, the following topological classification true*

a. if $\beta - d < \frac{ad}{K}$ then

i. E_1 is a sink if $0 < \delta < min\left\{\frac{2}{r}, \frac{2(a+K)}{ad+dK-K\beta}\right\}$,

ii. E_1 is a source if $\delta > max\left\{\frac{2}{r}, \frac{2(a+K)}{ad+dK-K\beta}\right\}$

iii. E_1 is a non-hyperbolic if $\delta = \frac{2}{r}$ or $\delta = \frac{2(a+K)}{ad+dK-K\beta}$.

b. if $\beta - d > \frac{ad}{K}$ *then*

i. E_1 *is a source if* $\delta > \frac{2}{r}$,

ii. E_1 *is a saddle if* $\delta < \frac{2}{r}$,

iii. E_1 *is a non-hyperbolic if* $\delta = \frac{2}{r}$.

c. if $\beta - d = \frac{ad}{K}$ *then* E_1 *is always non-hyperbolic.*

It is obvious that when $\delta = \frac{2}{r}$ or $\delta = \frac{2(a+K)}{ad+dK-K\beta}$, then one of the eigenvalues of $J(E_1)$ are $\lambda_1 = 1 - r\delta$ and $\lambda_2 = 1 - d\delta + \frac{K\beta\delta}{a+K}$is -1 and the other is not equal to ± 1. Therefore, a flip bifurcation can occur if parameters change in small vicinity of $FB^1_{E_1}$or $FB^2_{E_1}$:

$FB^1_{E_1} = \left\{(r, K, a, d, \delta) \in (0, +\infty): \delta = \frac{2}{r}, \delta \neq \frac{2(a+K)}{ad+dK-K\beta}, \beta - d < \frac{ad}{K}\right\}$,

or$FB^2_{E_1} = \left\{(r, K, a, d, \delta) \in (0, +\infty): \delta = \frac{2(a+K)}{ad+dK-K\beta}, \delta \neq \frac{2}{r}, \beta - d < \frac{ad}{K}\right\}$.

At $E_2(x^*, y^*)$, the Jacobian matrix (6) can be obtained as

$$J(E_2) = \begin{pmatrix} 1 - r\delta + \dfrac{dr\delta \ln\left(\frac{K(-d+\beta)}{ad}\right)}{\beta} & -\dfrac{d\alpha\delta}{\beta} \\ -\dfrac{r(d-\beta)\delta \ln\left(\frac{K(-d+\beta)}{ad}\right)}{\alpha} & 1 \end{pmatrix}$$

where

$trJ_{E_2} = 2 - r\delta + \frac{dr\delta \ln\left(\frac{K(-d+\beta)}{ad}\right)}{\beta}$,and $detJ_{E_2} = \frac{\beta - r\beta\delta + dr\delta(1 - d\delta + \beta\delta)\ln\left(\frac{K(-d+\beta)}{ad}\right)}{\beta}$.

Applying Jury's conditions, the fixed point E_2 is linearly asymptotically stable if and only if

$1 + trJ_{E_2} + detJ_{E_2} > 0$,
$1 - trJ_{E_2} + detJ_{E_2} > 0$,
$detJ_{E_2} - 1 > 0$.

Let $\mathrm{A}_1 = \frac{dr(-d+\beta)\ln\left(\frac{K(-d+\beta)}{ad}\right)}{\beta}$,$\mathrm{A}_2 = r\left(-1 + \frac{d\ln\left(\frac{K(-d+\beta)}{ad}\right)}{\beta}\right)$,$\mathrm{A}_3 = 4$,and $L = A_2^2 - A_1A_3$.

We state following proposition about stability criterion of E_2.

Proposition 2.2 *Suppose* $\beta - d > \frac{ad}{K}$. *Then the fixed point* $E_2(x^*, y^*)$ *of system (3) is a*

i. sink if one of the following conditions holds

(i.1) $L \geq 0 \quad and \quad \delta < \frac{-A_2-\sqrt{L}}{A_1}$;

(i.2) $L < 0 \quad and \quad \delta < -\frac{A_2}{A_1}$;

ii. source if one of the following conditions holds

(ii.1) $L \geq 0 \quad and \quad \delta > \frac{-A_2+\sqrt{L}}{A_1}$;

(ii.2) $L < 0 \quad and \quad \delta > -\frac{A_2}{A_1}$;

iii. non-hyperbolic if one of the following conditions holds

(iii.1) $L \geq 0 \quad and \quad \delta = \frac{-A_2 \pm \sqrt{L}}{A_1};\ \delta \neq -\frac{2}{A_2}, -\frac{4}{A_2}$

(iii.2) $L < 0 \quad and \quad \delta = -\frac{A_2}{A_1}$;

iv. saddle if otherwise.

From Proposition 2.3, we see that two eigenvalues of $J(E_2)$ are $\lambda_1 = -1$ and $\lambda_2 \neq \mp 1$ if condition (iii.1) holds. If (iii.2) is true, then the eigenvalues of $J(E_2)$ are complex having magnitude one.

Let

$$FB^1_{E_2} = \left\{(r, K, a, \alpha, \beta, d, \delta) \in (0, +\infty): \delta = \frac{-A_2 - \sqrt{L}}{A_1}, \quad L \geq 0, \delta \neq -\frac{2}{A_2}, -\frac{4}{A_2}\right\},$$

or

$$FB^2_{E_2} = \left\{(r, K, a, \alpha, \beta, d, \delta) \in (0, +\infty): \delta = \frac{-A_2 + \sqrt{L}}{A_1}, \quad L \geq 0, \delta \neq -\frac{2}{A_2}, -\frac{4}{A_2}\right\}.$$

Then system (3) experiences a flip bifurcation around fixed point E_2 if parameters vary in small vicinity of either set $FB^1_{E_2}$ or set $FB^2_{E_2}$.

Also let

$$NSB_{E_2} = \left\{(r, K, a, \alpha, \beta, d, \delta) \in (0, +\infty): \delta = -\frac{A_2}{A_1}, \quad L < 0\right\},$$

Then if the parameters change around the setNSB_{E_2}, system (3) experience a NS bifurcation atE_2.

3 Direction and Stability Analysis of Bifurcation

In this section, we will pay attention to determine the direction and stability of flip and NS bifurcations of system (3) around E_2 by using center manifold theory (Kuzenetsov, 1998). We set δ as a real bifurcation parameter.

3.1 Flip bifurcation

We take parameter $(r, K, a, \alpha, \beta, d, \delta)$ arbitrarily locate in $FB^1_{E_2}$. For the case of $FB^2_{E_2}$, one can do similar reasoning. Consider the system (3) at the fixed point $E_2(x^*, y^*)$ parameters lie in $FB^1_{E_2}$.

Let$\delta = \delta_F = \frac{-A_2-\sqrt{L}}{A_1}$, then the eigenvalues of $E_2(x^*, y^*)$ are$\lambda_1(\delta_F) = -1 \quad \text{and} \quad \lambda_2(\delta_F) = 3 + \mathrm{A}_2\delta_F$.

In order for $|\lambda_2(\delta_F)| \neq 1$, we have

$$A_2\delta_F \neq -2, -4 \tag{7}$$

We assume the transformation $\tilde{x} = x - x^*$, $\tilde{y} = y - y^*$ and write $A(\delta) = J(x^*, y^*)$. Then we shift the fixed point (x^*, y^*) of system (3) to the origin. After Taylor expansion, system (3) reduces to

$$\begin{pmatrix}\tilde{x}\\ \tilde{y}\end{pmatrix} \to A(\delta)\begin{pmatrix}\tilde{x}\\ \tilde{y}\end{pmatrix} + \begin{pmatrix}F_1(\tilde{x},\tilde{y},\delta)\\ F_2(\tilde{x},\tilde{y},\delta)\end{pmatrix} \tag{8}$$

where $X = (\tilde{x}, \tilde{y})^T$ is the vector of the transformed systemand

$$\begin{aligned} F_1(\tilde{x},\tilde{y},\delta) &= \frac{a\tilde{x}^2\alpha\delta(a\tilde{y}+\tilde{y}x^*-\tilde{x}y^*)}{(a+x^*)^4} - \frac{a\tilde{x}\alpha\delta(a\tilde{y}+\tilde{y}x^*-\tilde{x}y^*)}{(a+x^*)^3} + \frac{1}{6}\frac{r\tilde{x}^3\delta}{x^{*2}} + O(\| X \|^4) \\ F_2(\tilde{x},\tilde{y},\delta) &= -\frac{a\tilde{x}^2\beta\delta(a\tilde{y}+\tilde{y}x^*-\tilde{x}y^*)}{(a+x^*)^4} + \frac{a\tilde{x}\beta\delta(a\tilde{y}+\tilde{y}x^*-\tilde{x}y^*)}{(a+x^*)^3} + O(\| X \|^4) \end{aligned} \tag{9}$$

The system (8) can be expressed as

$$X_{n+1} = AX_n + \frac{1}{2}B(X_n, X_n) + \frac{1}{6}C(X_n, X_n, X_n) + O(\| X_n \|^4)$$

where $B(x,y) = \begin{pmatrix}B_1(x,y)\\ B_2(x,y)\end{pmatrix}$ and $(x,y,u) = \begin{pmatrix}C_1(x,y,u)\\ C_2(x,y,u)\end{pmatrix}$ are symmetric multi-linear vector functions of $x, y, u \in \mathbb{R}^2$ and defined as follows:

$$B_1(x,y) = \sum_{j,k=1}^{2} \left.\frac{\delta^2 F_1(\xi,\delta)}{\delta\xi_j\delta\xi_k}\right|_{\xi=0} x_j y_k = -\frac{rx_1y_1\delta}{x^*} - \frac{a\alpha\delta(ax_2y_1 + ax_1y_2 + x_2y_1x^* + x_1y_2x^* - 2x_1y_1y^*)}{(a+x^*)^3}$$

$$B_2(x,y) = \sum_{j,k=1}^{2} \left.\frac{\delta^2 F_2(\xi,\delta)}{\delta\xi_j\delta\xi_k}\right|_{\xi=0} x_j y_k = \frac{a\beta\delta(ax_2y_1 + ax_1y_2 + x_2y_1x^* + x_1y_2x^* - 2x_1y_1y^*)}{(a+x^*)^3},$$

$$C_1(x,y,u) = \sum_{j,k,l=1}^{2} \left.\frac{\delta^2 F_1(\xi,\delta)}{\delta\xi_j\delta\xi_k\delta\xi_l}\right|_{\xi=0} x_j y_k u_l = \frac{ru_1x_1y_1\delta}{x^{*2}} +$$

$$\frac{2a\alpha\delta(a(u_2x_1y_1+u_1x_2y_1+u_1x_1y_2)+u_2x_1y_1x^*+u_1(x_2y_1x^*+x_1y_2x^*-3x_1y_1y^*))}{(a+x^*)^4},$$

$$C_2(x,y,u) = \sum_{j,k,l=1}^{2} \left.\frac{\delta^2 F_2(\xi,\delta)}{\delta\xi_j\delta\xi_k\delta\xi_l}\right|_{\xi=0} x_j y_k u_l =$$

$$-\frac{2a\beta\delta(a(u_2x_1y_1 + u_1x_2y_1 + u_1x_1y_2) + u_2x_1y_1x^* + u_1(x_2y_1x^* + x_1y_2x^* - 3x_1y_1y^*))}{(a+x^*)^4},$$

and $\delta = \delta_F$.

Let $p, q \in \mathbb{R}^2$ be two eigenvectors of A for eigenvalue $\lambda_1(\delta_F) = -1$ such that $A(\delta_F)q = -q$ and $A^T(\delta_F)p = -p$. Then we have

$q \sim \left(2 - d\delta_F + \frac{\beta\delta_F x^*}{a+x^*}, -\frac{a\beta\delta_F y^*}{(a+x^*)^2}\right)^T$ and $p \sim \left(2 - d\delta_F + \frac{\beta\delta_F x^*}{a+x^*}, \frac{\alpha\delta_F x^*}{a+x^*}\right)^T$.

We use $\langle p,q\rangle = p_1q_1 + p_2q_2$,the standard scalar product in $\mathbb{R}^2$to normalize p,q such that $\langle p,q\rangle = 1$. To do, we set $p = \gamma_{\mathrm{F}}\left(2 - d\delta_F + \frac{\beta\delta_F x^*}{a+x^*}, \frac{\alpha\delta_F x^*}{a+x^*}\right)^T$, where

$$\gamma_{\mathrm{F}} = \frac{1}{\left(2 - d\delta_F + \frac{\beta\delta_F x^*}{a+x^*}, \frac{\alpha\delta_F x^*}{a+x^*}\right)^2 - \frac{a\alpha\beta\delta_F^2 x^* y^*}{(a+x^*)^3}}.$$

The sign of the coefficient of critical normal form$l_1(\delta_F)$ determines the direction of the flip bifurcation and is obtained as

$$l_1(\delta_F) = \frac{1}{6}\langle p, C(q,q,q)\rangle - \frac{1}{2}\langle p, B(q,(A-I)^{-1}B(q,q))\rangle \tag{10}$$

We state the following result on direction and stability of flip bifurcation according to above analysis.

Theorem 3.1 *If (7) holds,* $l_1(\delta_F) \neq 0$ *and the parameter* δ *changes its value in a small vicinity of* $FB^1_{E_2}$*, then system (3) undergoes a flip bifurcation around*$E_2(x^*, y^*)$*. Moreover, if* $l_1(\delta_F) > 0$ *(resp.,* $l_1(\delta_F) < 0$*) then the period-2 orbits that bifurcate from* $E_2(x^*, y^*)$ *are stable (resp., unstable).*

3.2 Neimark-Sacker bifurcation

Next, we take parameter $(r, K, a, \alpha, \beta, d, \delta)$arbitrarily locate in NSB_{E_2}. We consider system (3) at fixed point $E_2(x^*, y^*)$ with parameter$(r, K, a, \alpha, \beta, d, \delta) \in NSB_{E_2}$. Then the roots (eigenvalues) of equation (6), are pair of complex conjugate and given by $\lambda, \bar{\lambda} = \frac{-p(\delta) \pm i\sqrt{4q(\delta) - p(\delta)^2}}{2}$.

Let $\delta = \delta_{NS} = -\frac{A_2}{A_1}$ (11)

Therefore, we have$|\lambda| = \sqrt{q(\delta)}, \quad q(\delta_{NS}) = 1$.

From the transversality condition, we get

$$\frac{d|\lambda(\delta)|}{d\delta}\Big|_{\delta=\delta_{NS}} = -\frac{A_2}{2} \neq 0 \tag{12}$$

Moreover, nondegenerate condition $p(\delta_{NS}) \neq 0,1$, obviously satisfies

$$\frac{A_2^2}{A_1} \neq 2,3 \tag{13}$$

and we have

$$\lambda^k(\delta_{NS}) \neq 1 \quad \text{for } k = 1,2,3,4 \tag{14}$$

Suppose $q, p \in \mathbb{C}^2$ are two eigenvectors of $A(\delta_{NS})$ and $A^T(\delta_{NS})$ for eigenvalues $\lambda(\delta_{NS})$ and $\bar{\lambda}(\delta_{NS})$ such that

$$A(\delta_{NS})q = \lambda(\delta_{NS})q, \quad A(\delta_{NS})\bar{q} = \bar{\lambda}(\delta_{NS})\bar{q}$$

and

$$A^T(\delta_{NS})p = \bar{\lambda}(\delta_{NS})p, \quad A^T(\delta_{NS})\bar{p} = \lambda(\delta_{NS})\bar{p}.$$

By direct computation we obtain

$q \sim \left(1 - d\delta_{NS} + \frac{\beta\delta_{NS}x^*}{a+x^*} - \lambda, -\frac{a\beta\delta_{NS}y^*}{(a+x^*)^2}\right)^T$ and$p \sim \left(1 - d\delta_{NS} + \frac{\beta\delta_{NS}x^*}{a+x^*} - \bar{\lambda}, \frac{\alpha\delta_{NS}x^*}{a+x^*}\right)^T$.

For normalization of vectors p and q, we set $p = \gamma_{\mathrm{NS}}\left(1 - d\delta_{NS} + \frac{\beta\delta_{NS}x^*}{a+x^*} - \bar{\lambda}, \frac{\alpha\delta_{NS}x^*}{a+x^*}\right)^T$, where $\gamma_{\mathrm{NS}} = \frac{1}{\left(1-d\delta_{NS}+\frac{\beta\delta_{NS}x^*}{a+x^*}-\bar{\lambda}\right)^2 - \frac{a\alpha\beta\delta_{NS}^2x^*y^*}{(a+x^*)^3}}$.

Then it is clear that $\langle p, q\rangle = 1$ where $\langle p, q\rangle = \bar{p}_1 q_2 + \bar{p}_2 q_1$ for $p, q \in \mathbb{C}^2$. Now, we decompose vector $X \in \mathbb{R}^2$as $X = zq + \bar{z}\bar{q}$, for δ close to δ_{NS} and $z \in \mathbb{C}$. Obviously, $z = \langle p, X\rangle$. Thus, we obtain the following transformed form of system (8) for $|\delta|$near δ_{NS}:

$$z \mapsto \lambda(\delta)z + g(z, \bar{z}, \delta),$$

where $\lambda(\delta) = (1 + \varphi(\delta))e^{i\theta(\delta)}$ with $\varphi(\delta_{NS}) = 0$ and $g(z, \bar{z}, \delta)$ is a smooth complex-valued function. After Taylor expression of g with respect to $(z, \bar{z})$, we obtain

$$g(z, \bar{z}, \delta) = \sum_{k+l\geq 2} \frac{1}{k!\, l!} g_{kl}(\delta) z^k \bar{z}^l, \quad \text{with} \quad g_{kl} \in \mathbb{C}, \qquad k, l = 0,1, \cdots.$$

According to multilinear symmetric vector functions, the coefficients g_{kl} are

$$g_{20}(\delta_{NS}) = \langle p, B(q, q)\rangle, \quad g_{11}(\delta_{NS}) = \langle p, B(q, \bar{q})\rangle$$
$$g_{02}(\delta_{NS}) = \langle p, B(\bar{q}, \bar{q})\rangle, \quad g_{21}(\delta_{NS}) = \langle p, C(q, q, \bar{q})\rangle,$$

The coefficient $l_2(\delta_{NS})$ which determines the direction of NS bifurcationin a generic system exhibiting invariant closed curve can be calculated via

$$l_2(\delta_{NS}) = \mathrm{Re}\left(\frac{e^{-i\theta(\delta_{NS})}g_{21}}{2}\right) - \mathrm{Re}\left(\frac{(1 - 2e^{i\theta(\delta_{NS})})e^{-2i\theta(\delta_{NS})}}{2(1 - e^{i\theta(\delta_{NS})})} g_{20}g_{11}\right) - \frac{1}{2}|g_{11}|^2 - \frac{1}{4}|g_{02}|^2,$$

where $e^{i\theta(\delta_{NS})} = \lambda(\delta_{NS})$.

Summarizing above analysis, we present the following theorem for direction and stability of NS bifurcation.

Theorem 3.2 *If (13) holds, $l_2(\delta_{NS}) \neq 0$ and the parameter δ changes its value in small vicinity of NSB_{E_2}, then system (3) passes through a Neimark-Sacker bifurcation around E_2. Moreover, if $l_2(\delta_{NS}) < 0$ (resp.,> 0), then there exists a unique attracting (resp., repelling) invariant closed curve bifurcates from E_2.*

Table 1 Parameter values.

Cases	***Varying parameter in range***	***Fixed parameters***	***System Dynamics***
Case (i)	$2.15 \leq \delta \leq 2.88$	$r = 1.75, K = 1.0, a = 0.4, \alpha = 0.5, \beta = 0.05, d = 0.01$	FB
Case (ii)	$1.8 \leq \delta \leq 2.95$	$r = 1.25, K = 1.05, a = 0.3, \alpha = 0.5, \beta = 0.4, d = 0.15$	NS
Case (iii)	$0.248 \leq a \leq 0.32$	$r = 1.25, K = 1.05,$ $\alpha = 0.5, \beta = 0.4, d = 0.15, \delta = 2.04827$	NS

4 Numerical Simulations

In this section, numerical simulation are performed to validate our theoretical results, especially, we present bifurcation diagrams of system (3) around E_2, phase portraits, maximum Lyapunov exponents and fractal dimension corresponding to bifurcation diagrams. We assume that δ is a real bifurcation parameter unless stated. We consider different set of parameter values for bifurcation analysis as given in Table 1.

Example 1: Flip bifurcation of system (3) with respect to bifurcation parameter δ.

We set values of parameter as given incase (i). By calculation, we obtain a unique fixed point $E_2(0.1, 4.02952)$ of system (3). The critical point for FB is $\delta_F \sim 2.20115$. It is observed that the system (3) experiences a FB around E_2 when δ passes its critical value δ_F.At$\delta = \delta_F$, the two eigenvalues are $\lambda_1 = -1, \lambda_2 = 0.921907$, $l_1(\delta_F) = 349.055$and $(r, K, a, \alpha, \beta, d, \delta) \in FB^1_{E_2}$. This verifies Theorem 3.1.

The bifurcation diagrams shown in Fig. 1(a-b) reveal that stability of fixed point E_2 happens for $\delta < \delta_F$, at $\delta = \delta_F$ system (3) loses its stability and for $\delta > \delta_F$ there exists a period doubling phenomena leading to chaos. There exists period -2,-4, -8orbits occur for the window $\delta \in [2.1, 2.7942]$ and chaotic set for $\delta \in [2.7942, 2.88]$. The MLEs and FD related to Fig. 1(a-b) are computed and displayed in Fig. 1(c-d). The status of stable, periodic or chaotic dynamics are compatible with sign of MLE as in Fig. 1(c-d). The phase portraits of bifurcation diagrams in Fig. 2(a-b) for different values of δ are displayed in Fig. 2.

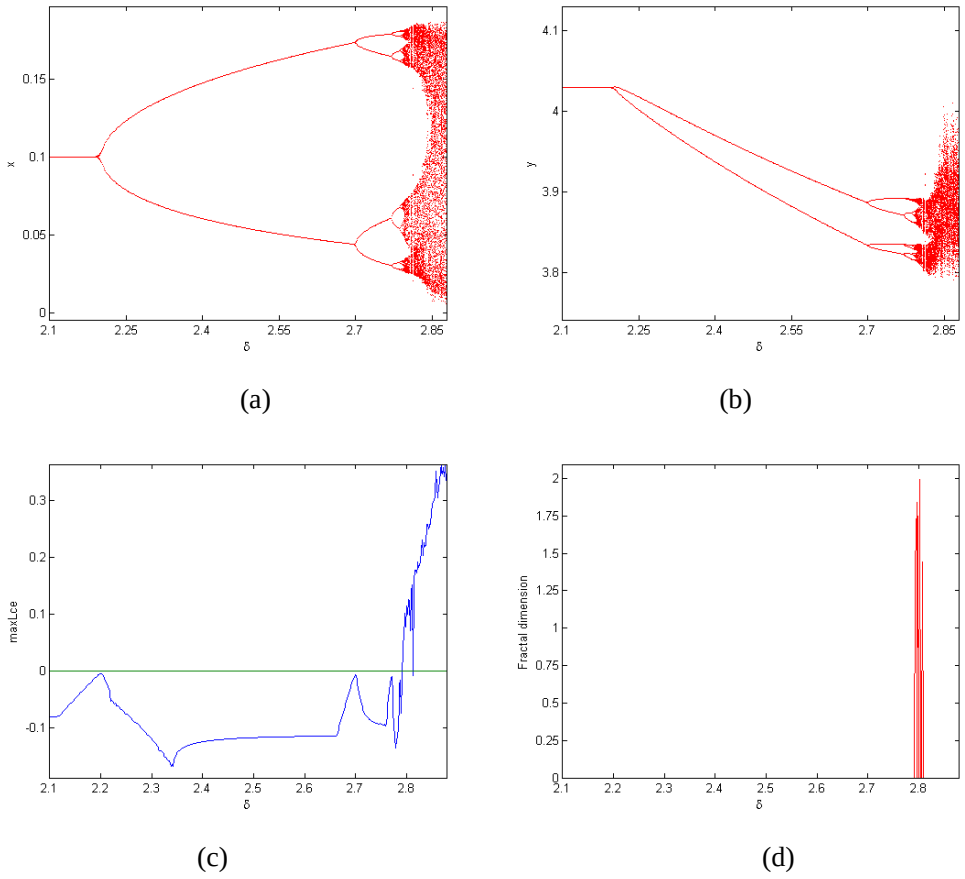

(a) (b)

(c) (d)

Fig. 1 Flip bifurcation and Lyapunov exponent of system (3). (a) FB in prey, (b) FB in predator, (c) MLEs related to (a-b), (d) FD corresponding to (a). Initial value $(x_0, y_0) = (0.1, 4.02)$.

Example 2: NS bifurcation of system (3) with respect to bifurcation parameter δ.

With the variation of parameter δ, the system (3) exhibits much richerdynamics through the emergence of NS bifurcation. We take parameters as given in case (ii). After calculation, we find a unique fixed point $E_2(0.18, 2.11631)$. A NS bifurcation point is obtained as$\delta = \delta_{NS} \sim 2.04827$. It is shown that the system (3) experiences a NS bifurcation around E_2 when δ passes its critical value δ_{NS}. Also at $\delta = \delta_{NS}$ we

have $\lambda, \bar{\lambda} = 0.566465 \pm 0.824086\, i$, $g_{20} = 0.135473 + 0.245758\, i$, $g_{11} = 2.2689 - 0.906715\, i$, $g_{02} = -1.25699 + 4.9813\, i$, $g_{21} = -4.96799 + 6.72114\, i$, and $l_2(\delta_{NS}) = -8.120394164511106$. It is obvious that $(r, K, a, \alpha, \beta, d, \delta) \in NSB_{E_2}$. This verifies the correctness of Theorem 3.2.

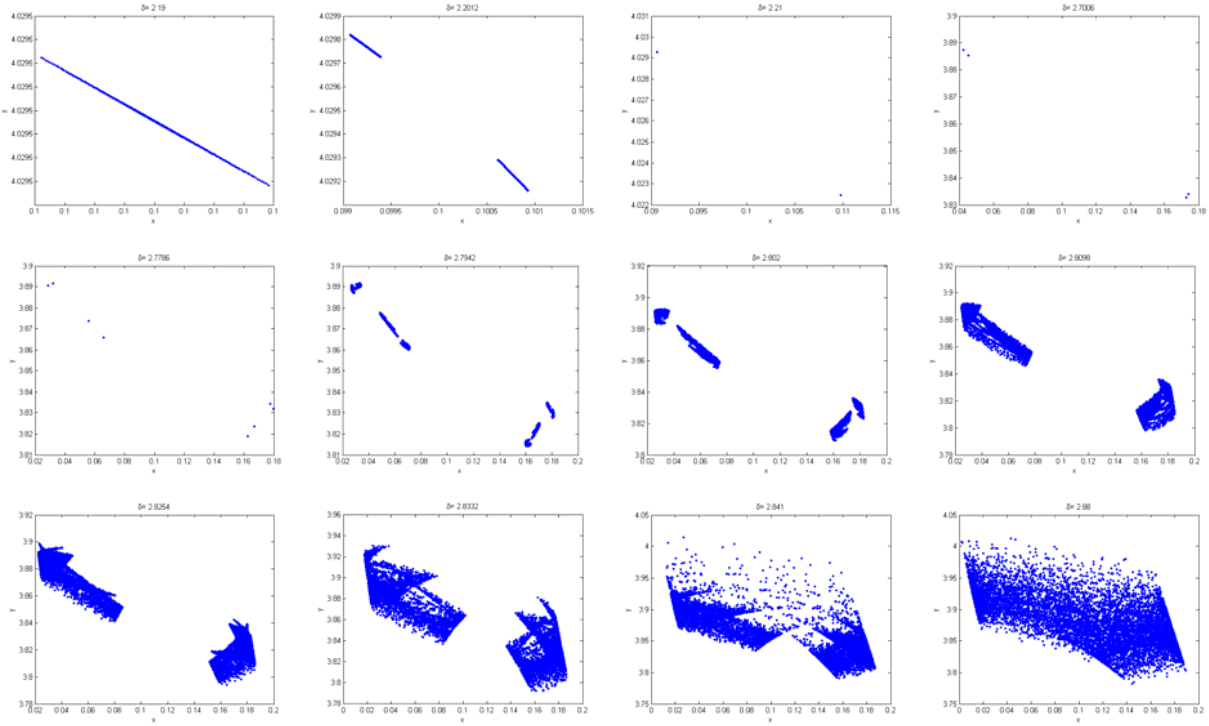

Fig. 2 Phase portraits (xy-plane) of bifurcation diagrams Fig. 1(a-b) for different values of δ.

The bifurcation diagrams shown in Fig. 3(a-b) demonstrate that $E_2$is stabile for$\delta < \delta_{NS}$, loses its stability at $\delta = \delta_{NS}$ and an attracting invariant curve appears if $\delta > \delta_{NS}$. We dispose the MLEs in Fig. 3(c) relating bifurcation in Fig. 3(a-b), which confirm the existences of chaos and periodic orbits as parameter δ varying. These results indicate that NS bifurcation instigates a route to chaos, through a dynamic transition from a stable state, to invariant closed cycle, with periodic and quasi-periodic states occurring in between, to chaotic sets. For instance, when $\delta \sim 2.95$, the sign of MLE confirming presence of chaos. Fig. 3(d) is local amplification of Fig. 3(a) for $\delta \in [2.75, 2.95]$.

The phase portraits of bifurcation diagrams in Fig. 3(a-b) for different values of δ are displayed in Fig. 4, which clearly illustrates the act of smooth invariant curve how it bifurcates from the stable fixed point and increases its radius. As δ grows, disappearance of closed curve occurs suddenly and a period-6, -11, -20, -10, -5 and period -25 orbits appear at $\delta \sim 2.283$, $\delta \sim 2.582$, $\delta \sim 2.835, \delta \sim 2.858, \delta \sim 2.8925$, and $\delta \sim 2.9155$ respectively. We also see that a fully developed chaos in system (2) occurs at $\delta \sim 2.95$.

Example 3: NS bifurcation of system (3) with respect to bifurcation parameter a.

With the variation of other parameter values (e.g., parameter a), the predator-prey system (3) may exhibit another richer dynamical behaviors. When we set the parameter values as given in case (iii), a new NS bifurcation diagram is obtained as disposed in Fig. 5(a-b). The system firstly enters chaotic dynamics for small value of a. However, with the increase of a value, the chaotic dynamics of the system suddenly disappear

through a NS bifurcation occurring first at$a = a_{NS}$~0.3. Similar nonlinear characteristics to Figures 3 and 4 are found in this case, such as route to chaos, invariant curves, chaotic attractors, periodic and quasi-periodic states. The MLE corresponding to Fig. 5(a-b) is computed and plotted in Fig. 5(c), which confirm the existences of chaos and periodic orbit as parameter a varying. We notice that system dynamics is stable if $a > a_{NS}$, loses its stability at $a = a_{NS}$ and an attracting invariant closed curve appears if $a < a_{NS}$. That is decreased values of parameter a causes complex system dynamics which trigger a route to chaos via NS bifurcation. As $a$decreases, closed curve suddenly disappear and a period -7, -14, and -28 orbits and attracting chaotic sets appear at a~0.2562, a~0.2542, a~0.2528 and a~0.249 respectively.

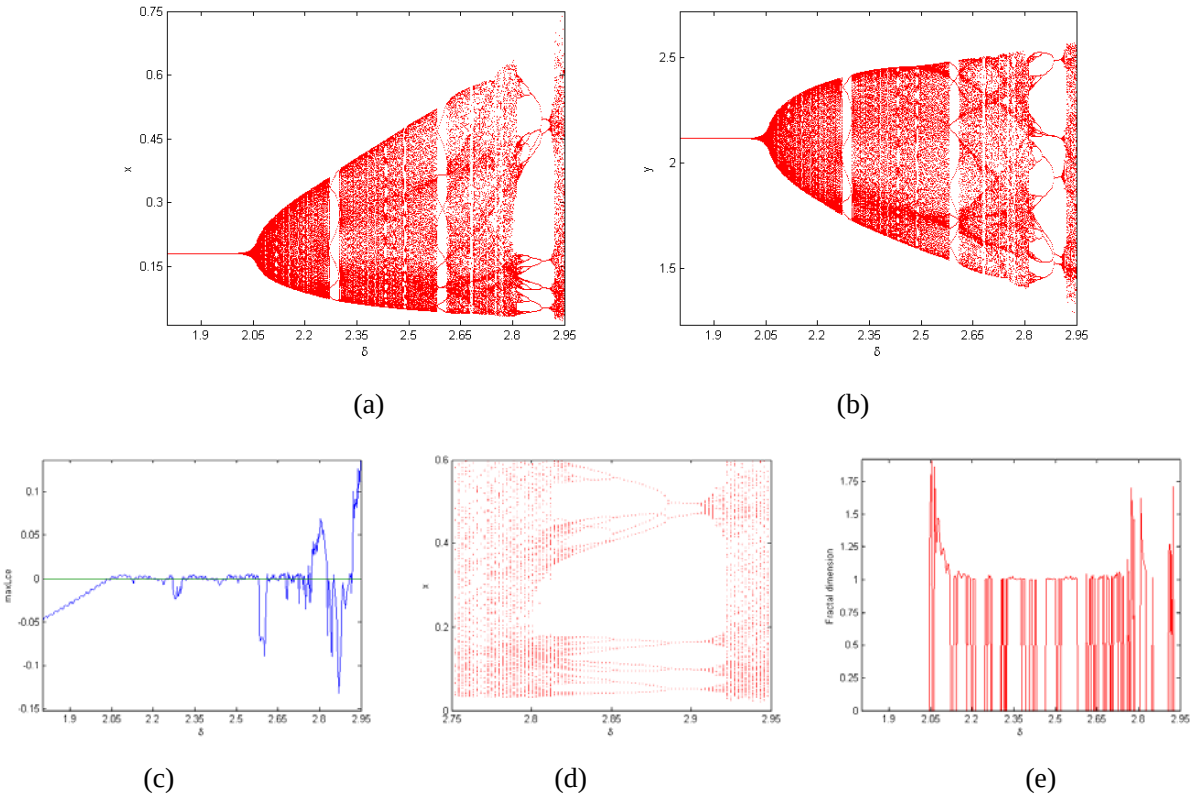

Fig. 3 NS bifurcation and Lyapunov exponent of system (3). (a) NS bifurcation in prey, (b) NS bifurcation in predator, (c) MLEs related to (a-b), (d) local amplification of (a) for $\delta \in [1.8,2.95]$ (e) FD associated with (a). Initial value $(x_0, y_0) = (0.17,2.11)$.

Example 4: Parametric basins of attractions.

When two more parameters change through its critical values, then system (3) can exhibit more complex dynamic behavior. Ina 2D parameter space the parametric basins of attraction (Gkana, 2013) is plotted to notice how the system dynamics qualitatively change as parameter values increase. This plot (Fig. 6) is a numerical analysis tool in which the different colors describe different stability states. So, we first plot (Fig. 6a) the parametric basins of attraction for the parameter values $a \in [0248, 0.32]$ and $\beta \in [0.35, 0.5]$ and rest of parameter values as in case (ii) or case (iii). Fig. 6b is the plot in the parametric plane (a, δ) with $a \in [0248, 0.32]$ and $\delta \in [1.8, 2.95]$. Fig. 6b is the plot in the parametric plane (β, K) with $\beta \in [0.35, 0.5]$ and $K \in [1.0, 1.258]$. It is simple to find values of control parameters for which the dynamics of system (3) is in

status of non-chaotic, periodic or chaotic. The red and blue regions for an attracting fixed point and/or for stable periodic cycles. The white region corresponds to those parameters values for which the solution trajectories may be quasi-periodic (invariant curves) or non-periodic (chaos, strange attractors). The black region is the set of parameters for which the solution trajectories diverge to infinity.

From 2D parameter space (Fig. 6) we observe the following:

- The increases values of control parameters a and β, the solution behaviors of system (3) change from non-periodic to an attracting fixed point or stable periodic cycle.
- The increases values of control parameters a and δ, the dynamics of system (3) change from chaotic to non-chaotic states.
- The increases values of control parameters β and K, the system dynamics significantly change from non-chaotic to chaotic states.

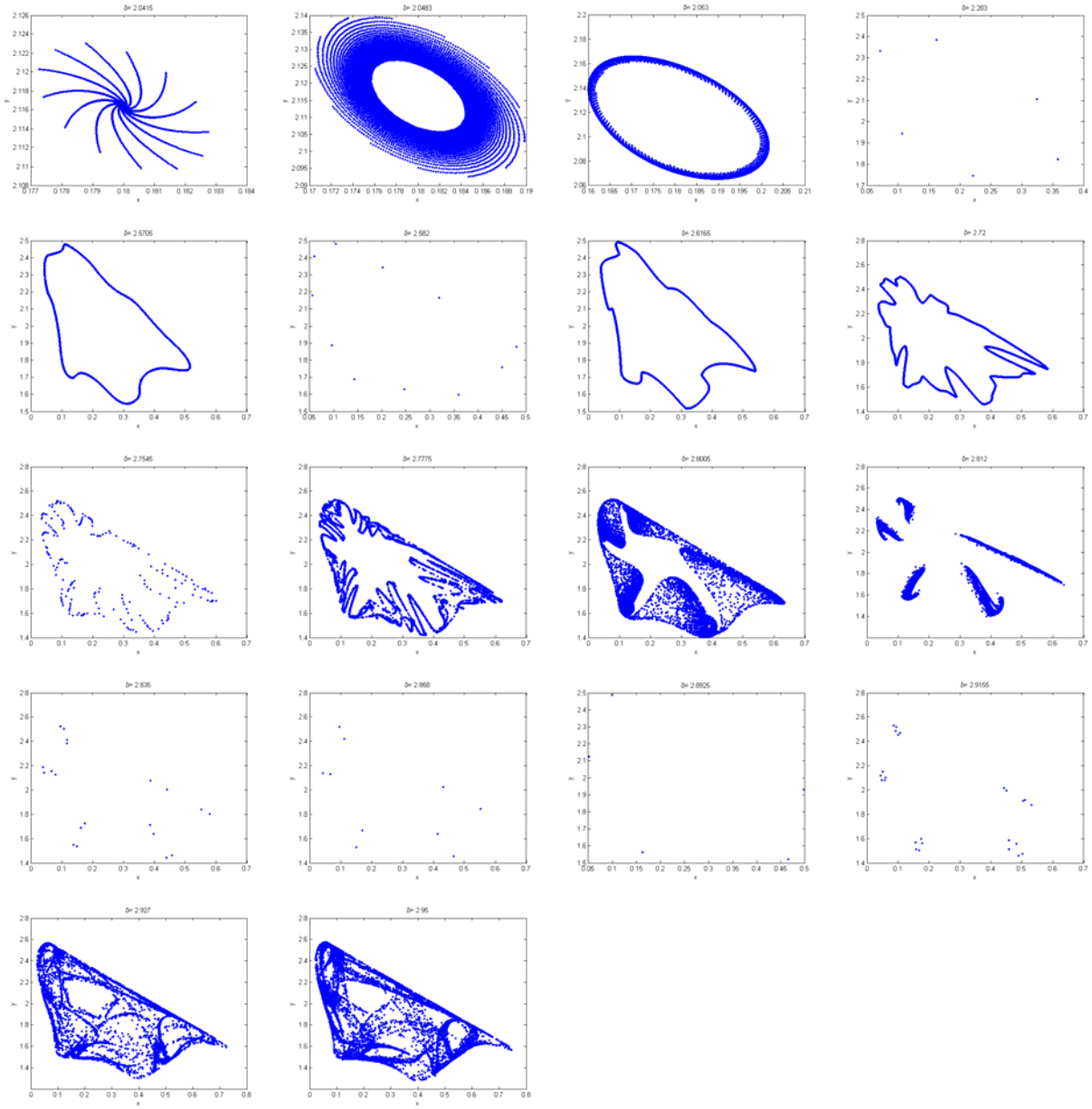

Fig. 4 Phase portraits (xy-plane) of bifurcation diagrams Fig. 3(a-b) for different values of δ.

Fractal dimension of system (3)

The measure of fractal dimensions characterizes the strange attractors of a system. By using Lyapunov exponents, the fractal dimension (Cartwright, 1999; Kaplan and Yorke, 1979) is defined by

$$d_L = j + \frac{\sum_{i=1}^{j} h_i}{|h_j|}$$

where $h_1, h_2, \ldots, h_n$ are Lyapunov exponents and j is the largest integer such that $\sum_{i=1}^{j} h_i \geq 0$ and $\sum_{i=1}^{j+1} h_i < 0$.

For our two-dimensional system (3), the fractal dimension takes the form

$$d_L = 1 + \frac{h_1}{|h_2|}, \quad h_1 > 0 > h_2 \text{ and } h_1 + h_2 < 0.$$

With parameter values as in case (ii), the fractal dimension of system (3) is plotted in Fig. 3(e). The strange attractors given in Fig. 4 and its corresponding FD illustrate that the increase values of parameter δ causes a chaotic dynamics for the predator-prey system (3).

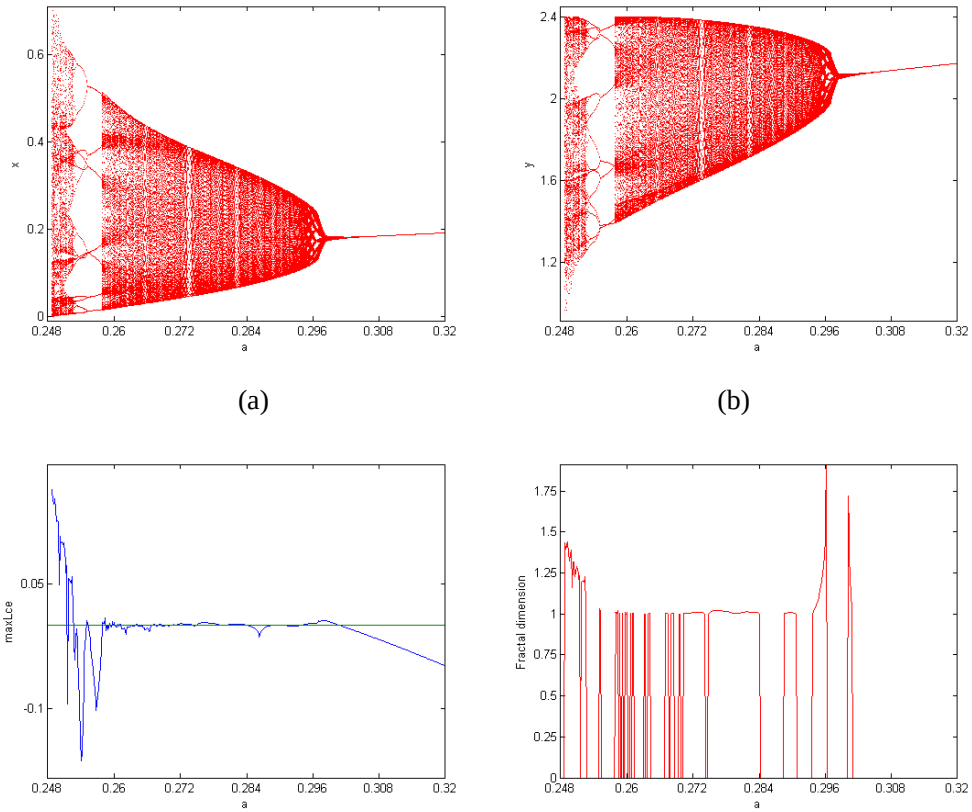

(a) (b)

(c) (d)

Fig. 5 NS bifurcation and Lyapunov exponent of system (3). (a) NS bifurcation in prey, (b) NS bifurcation in predator, (c) MLEs related to (a-b), (d) FD associated with (a). Initial value $(x_0, y_0) = (0.17, 2.11)$.

5 Chaos Control

To stabilize chaos at the state of unstable trajectories of system (3), a state feedback control method (Elaydi, 1996) is applied. By adding a feedback control law as the control force u_n to system (3), the controlled form

of system (3) becomes

$$\begin{aligned} x_{n+1} &= x_n + \delta\left[rx_n \ln\left(\frac{K}{x_n}\right) - \frac{ax_n}{a+x_n}y_n\right] + u_n \\ y_{n+1} &= y_n + \delta\left[\frac{\beta x_n}{a+x_n}y_n - dy_n\right] \end{aligned} \tag{15}$$

and

$u_n = -k_1(x_n - x^*) - k_2(y_n - y^*)$ where k_1 and k_2 are the feedback gains and (x^*, y^*) represent positive fixed point of system (3). The Jacobian matrix J_c of the controlled system (15) is given by

$$J_c(x^*, y^*) = \begin{pmatrix} j_{11} - k_1 & j_{12} - k_2 \\ j_{21} & j_{22} \end{pmatrix} \tag{16}$$

where $j_{pq}, p, q = 1,2$ given in (5) are evaluated at (x^*, y^*). The characteristic equation of (16) is

$$\lambda^2 - (trJ_c)\lambda + detJ_c = 0 \tag{17}$$

where $trJ_c = j_{11} + j_{22} - k_1$ and $detJ_c = j_{22}(j_{11} - k_1) - j_{21}(j_{12} - k_2)$. Let λ_1 and λ_2 be the roots of (17). Then

$$\lambda_1 + \lambda_2 = j_{11} + j_{22} - k_1 \tag{18}$$

and

$$\lambda_1\lambda_2 = j_{22}(j_{11} - k_1) - j_{21}(j_{12} - k_2) \tag{19}$$

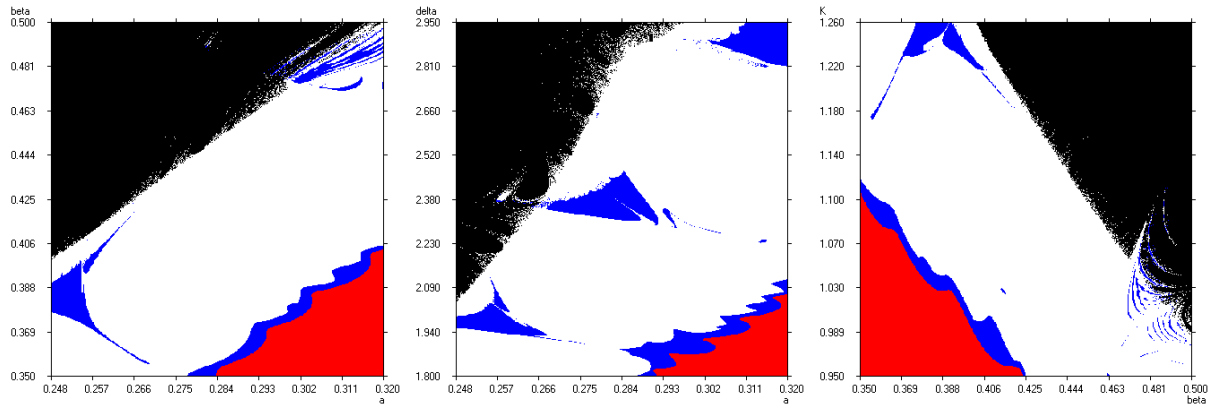

Fig. 6 Diagnostic of system (3) in a 2D parameter space. (a) parametric basins of attraction in (a, β)-plane (b) parametric basins of attraction in (a, δ)-plane (c) parametric basins of attraction in(β, K)-plane.

The solution of the equations $\lambda_1 = \pm 1$ and $\lambda_1\lambda_2 = 1$ determines the lines of marginal stability. These conditions confirm that $|\lambda_{1,2}| < 1$. Suppose that $\lambda_1\lambda_2 = 1$, then from (19) we have

$$l_1: j_{22}k_1 - j_{21}k_2 = j_{11}j_{22} - j_{12}j_{21} - 1.$$

Assume that $\lambda_1 = 1$, then from (18) and (19) we get

$$l_2: (1 - j_{22})k_1 + j_{21}k_2 = j_{11} + j_{22} - 1 - j_{11}j_{22} + j_{12}a_{21}.$$

Next, assume that $\lambda_1 = -1$, then from (18) and (19) we obtain

$$l_3: (1 + j_{22})k_1 - j_{21}k_2 = j_{11} + j_{22} + 1 + j_{11}j_{22} - j_{12}j_{21}.$$

We determine a triangular region in the (k_1, k_2)-plane by plotting the lines $l_1, l_2,$ and l_3 (see Fig. 7(a)) which keeps eigenvalues with magnitude less than 1. In order to check how the implementation of feedback control method works and controls chaos at unstable trajectories, we have carried out numerical simulations.

With fixed $\delta = 2.95$ and rest parameters as in case (ii), we consider the feedback gains are as$k_1 = 1.05$ and $k_2 = -0.35$. The initial value is $(x_0, y_0) = (0.17,2.11)$ and Fig.7(b) and 7(c) show that at the fixed point $(0.18, 2.11631)$, the chaotic trajectory is stabilized.

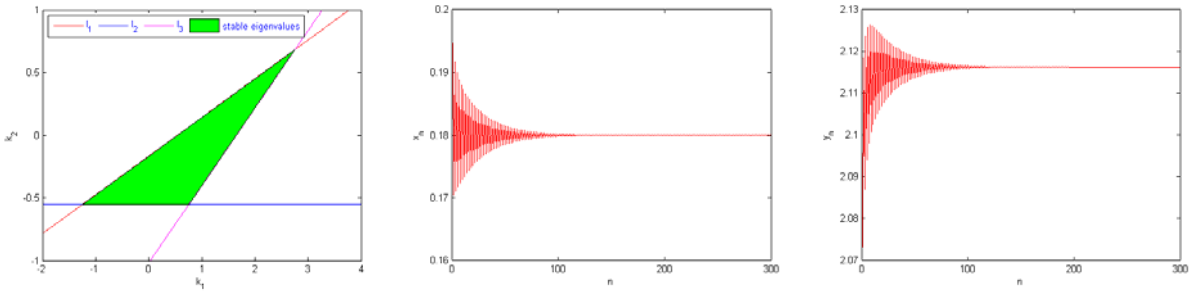

(a) (b) (c)

Fig. 7 Control of chaotic trajectories of system (15). (a) Stability region in (k_1, k_2) plane (b-c) Time series for states x and y respectively.

6 Discussions

This work is concerned with the dynamics of a discrete-time predator-prey system with Michaelis-Menten functional response and Gompertz growth of prey in the closed first quadrant $\mathbb{R}^2_+$. By the center manifold theory, we determine the existence condition and direction of flip and NS bifurcations of system (3) around E_2. In particular, we show that the system (3) can undergo a flip and NS bifurcation at unique fixed pointE_2 if δ varies around the sets $FB^1_{E_2}$ or $FB^2_{E_2}$ and NSB_{E_2}. Based on Figures, we notice that the small integral step size δ can stabilize the dynamical system (3), but the large integral step size may destabilize the system producing more complex dynamical behaviors. In addition, we see that the appropriate choice of the half saturation parameter a can stabilize the dynamical system (3). However, for the low values of a destabilize system (3).Numerical simulations present unpredictable behaviors of the system through a flip bifurcation which include orbits of period-2, -4, -8orbits and through a NS bifurcation which include an invariant cycle, orbits of period -5, -6, -7, -10, -11, -14, -20, -25 and period -28 orbits and chaotic sets respectively. These indicate that at the state of chaos, the system is unstable and particularly, the predator goes to extinct or goes to a stable fixed point when the dynamic of prey is chaotic. We confirm about the existence of chaos through the computation of MLEs and FD. The two bifurcations (FB and NSB) both trigger a route to chaos via periodic and quasi-periodic states; that is, chaotic dynamics appear or disappear along with the emergence of bifurcations. Moreover, we plot the parametric basins of attraction for system (3) by the variation of two control parameters. This plot exhibits very rich nonlinear dynamical behaviors and one can directly observe from this 2D parametric space when the system dynamics will be periodic, quasi-periodic and chaotic. Finally, the chaotic trajectories at unstable state are controlled by implementing the strategy of feedback control. In future, we would expect to obtain more analytical results on multiple parameter bifurcation exist in the system.

References

Berryman AA. 1992. The origins and evolution of predator-prey theory. Ecology, 73: 15301535

Cartwright JHE. 1999. Nonlinear stiffness Lyapunov exponents and attractor dimension. Physics Letters A, 264: 298–304

Elaydi SN. 1996. An Introduction to Difference Equations. Springer-Verlag, New York, USA

Freedman HI. 1980. Deterministic Mathematical Models in Population Ecology. Marcel Dekker, New York, USA

Gkana A, Zachilas L. 2013. Incorporating prey refuge in a prey–predator model with a Holling type I functional response random dynamics and population outbreaks. Journal of Biological Physics, 39: 587-606

Gompertz B. 1825. On the nature of the function expressive of the law of human mortality. Philosophycal Transactions of Royal Society, 115: 513-585

He ZM, Lai X. 2011. Bifurcation and chaotic behavior of a discrete-time predator-prey system. Nonlinear Analysis: Real World Applications, 12: 403-417

He ZM, Li B. 2014. Complex dynamic behavior of a discrete-time predator-prey system of Holling-III type. Advances in Difference Equations, 180

Liu, W, Cai D. 2019. Bifurcation, chaos analysis and control in a discrete-time predator-prey system. Advances in Difference Equations, 11

Kaplan JL, Yorke YA. 1979. A regime observed in a fluid flow model of Lorenz. Communications in Mathematical Physics, 67: 93-108

Kuzenetsov YA. 1998. Elements of Applied Bifurcation Theory (2nd Ed). Springer-Verlag, New York, USA

May RM. 1974. Stability and Complexity in Model Ecosystems. Princeton University Press, USA

Rana SMS. 2015. Bifurcation and complex dynamics of a discrete-time predator-prey system with simplified Monod-Haldane functional response. Advances in Difference Equations, 345

Rana SMS, Kulsum U. 2017. Bifurcation analysis and chaos control in a discrete-time Predator-Prey System of Leslie Type with Simplified Holling Type IV Functional Response. Discrete Dynamics in Nature and Society, Special Issue

Rana SMS. 2017. Chaotic dynamics and control of discrete ratio-dependent predator-prey system. Discrete Dynamics in Nature and Society, 4537450: 1-13

Rana SMS. 2019. Bifurcations and chaos control in a discrete-time predator-prey system of Leslie type. Journal of Applied Analysis and Computation, 9(1): 31-44

Rana SMS. 2019. Dynamics and chaos control in a discrete-time Holling-Tanner model. Journal of the Egyptian Mathematical Society, 27: 48

Zhao M, Xuan Z, Li C. 2016. Dynamics of a discrete-time predator-prey system. Advances in Difference Equations, 191

Zhao M, Li C, Wang J. 2017. Complex dynamic behaviors of a discrete-time predator-prey system. Journal of Applied Analysis and Computation, 7: 478-500